Electronic Supplementary Material (ESI) for New Journal of Chemistry.

Supporting Information for "*Thermally-induced spin-crossover (SCO) in Fe(4-Ethynylpyrdine)$_2$[Fe(CN)$_5$NO]. Why is the SCO observed in 2D ferrous nitroprussides despite the NO-NC repulsive interaction in the interlayer region*?" by Karla Scanda, Yosuan Avila, Laritza Sánchez, Rodrigo Mojica, Marlene González, Beatriz D. Moreno, Manuel Avila, and Edilso Reguera.

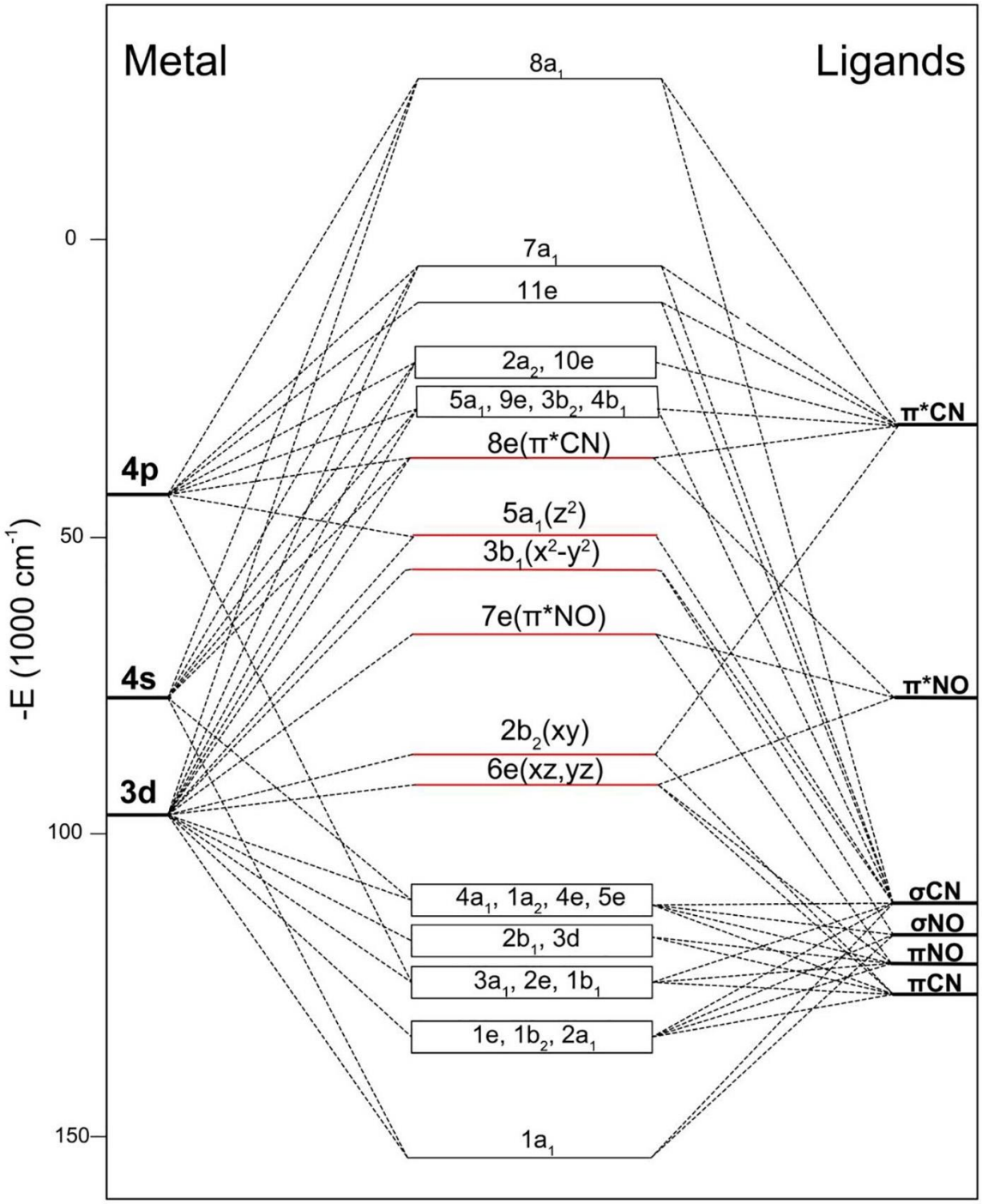

Figure S1. Molecular orbital energy levels for nitroprusside ion, $[Fe(CN)_5NO]^{2-}$. Reproduced from P.T. Manoharan, H.B. Gray, J. Am. Chem. Soc. 87 (1965) 3340.

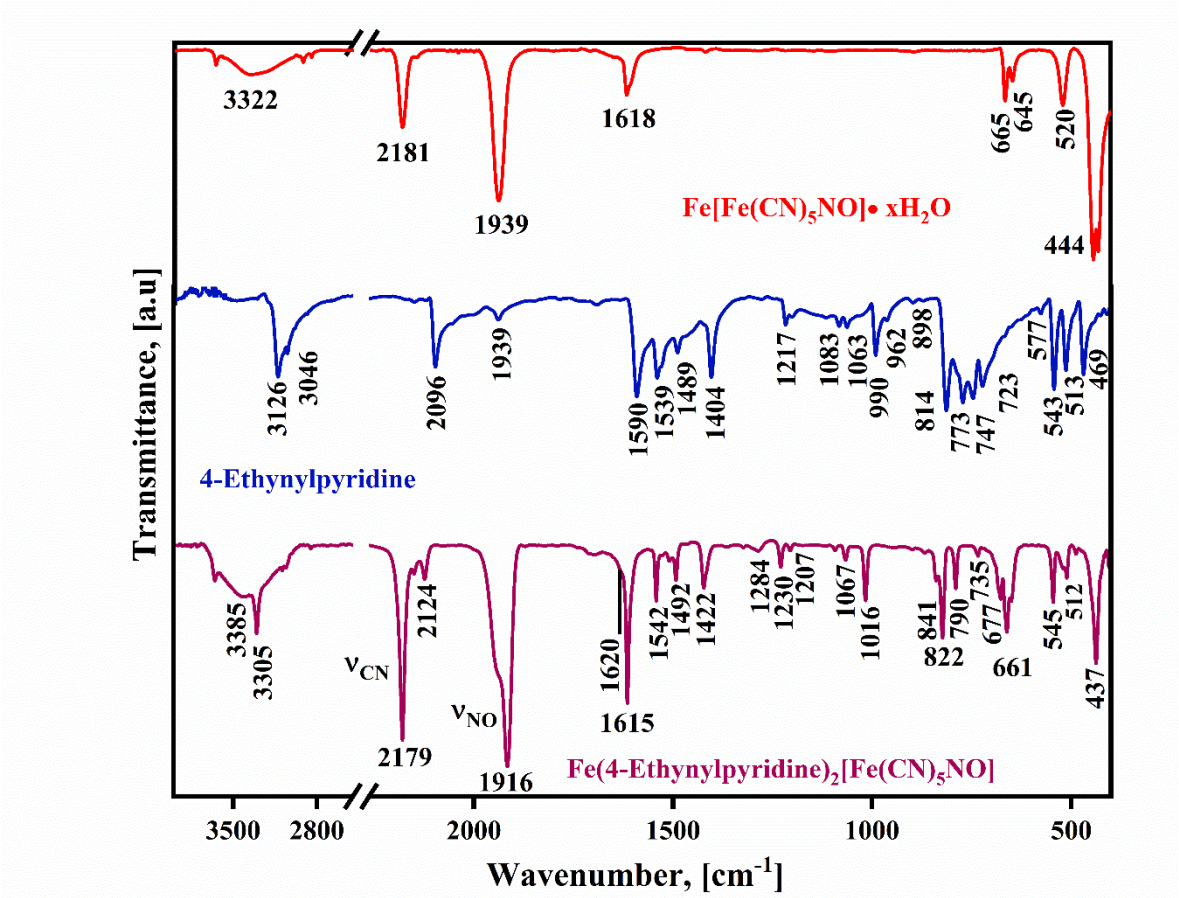

Figure S2. IR spectra of ferrous nitroprusside (3D cubic phase), 4-Ethynylpyridine, and the solid formed by sonicating a suspension of 3D ferrous nitroprusside and the molecule in a 1:2 molar ratio.

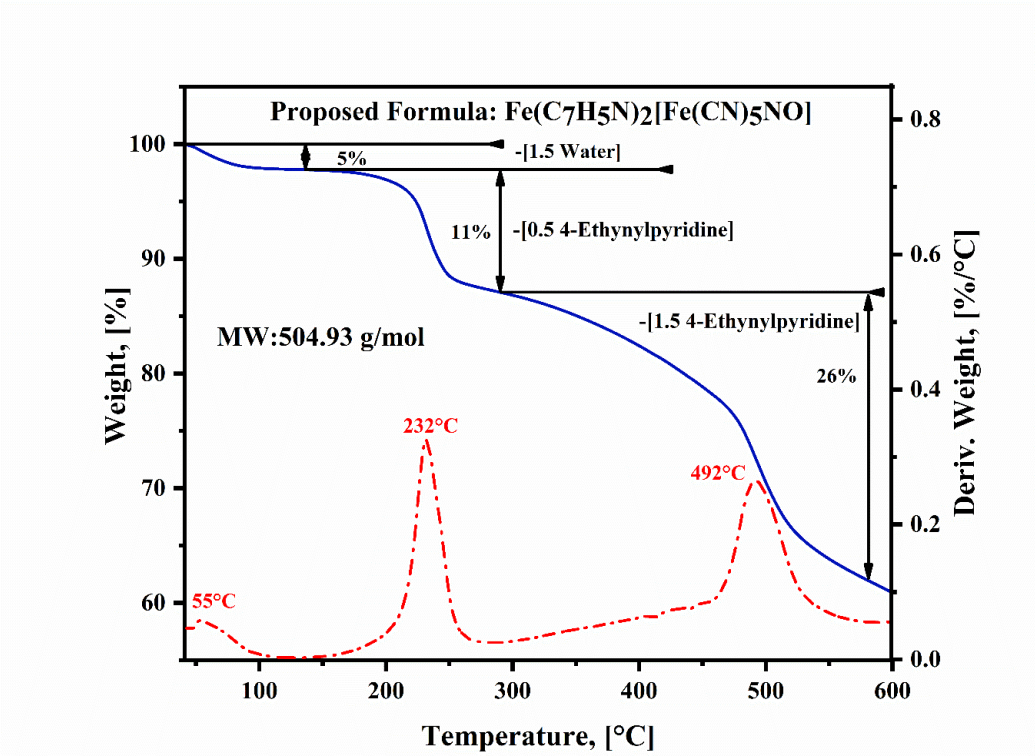

Figure S3. TG curves of IR spectra of ferrous nitroprusside (3D cubic phase), 4-Ethynylpyridine, and the solid formed by sonicating a suspension of 3D ferrous nitroprusside and the molecule in a 1:2 molar ratio.

Table S1. Frequency for the main characteristic IR absorption bands of $Fe(4\text{-}EPy)_2[Fe(CN)_5NO]$ at 298 K.

TA	77 K	Assignment
3305	3310	ν(C-H) EPy
2179	2188	ν(C≡N) CN_{Eq}
1911	1916	ν(N=O) Nitrop.
1615	1618	ν(C-C) EPy
1542	1542	$\nu(CN)_{ring}$ EPy
1016	1023	ν,ρ (ring) EPy
822	824	ω (ring) EPy
661	661	δ(H-C-C) EPy
545	552	δ[Fe-C≡N_{Eq}]

Table S2. Results for the elemental chemical analysis for the material under study as an anhydrous phase.

Sample	%Fe		%C		%N		%O		%H	
	Cal.	Exp.	Cal.	Exp.	Cal.	Exp.	Cal.	Exp.	Cal.	Exp.
$Fe(C_7H_5N)_2[Fe(CN)_5NO]$	28.35	28.40	36.58	36.23	28.44	28.37	4.06	4.11	2.55	2.59

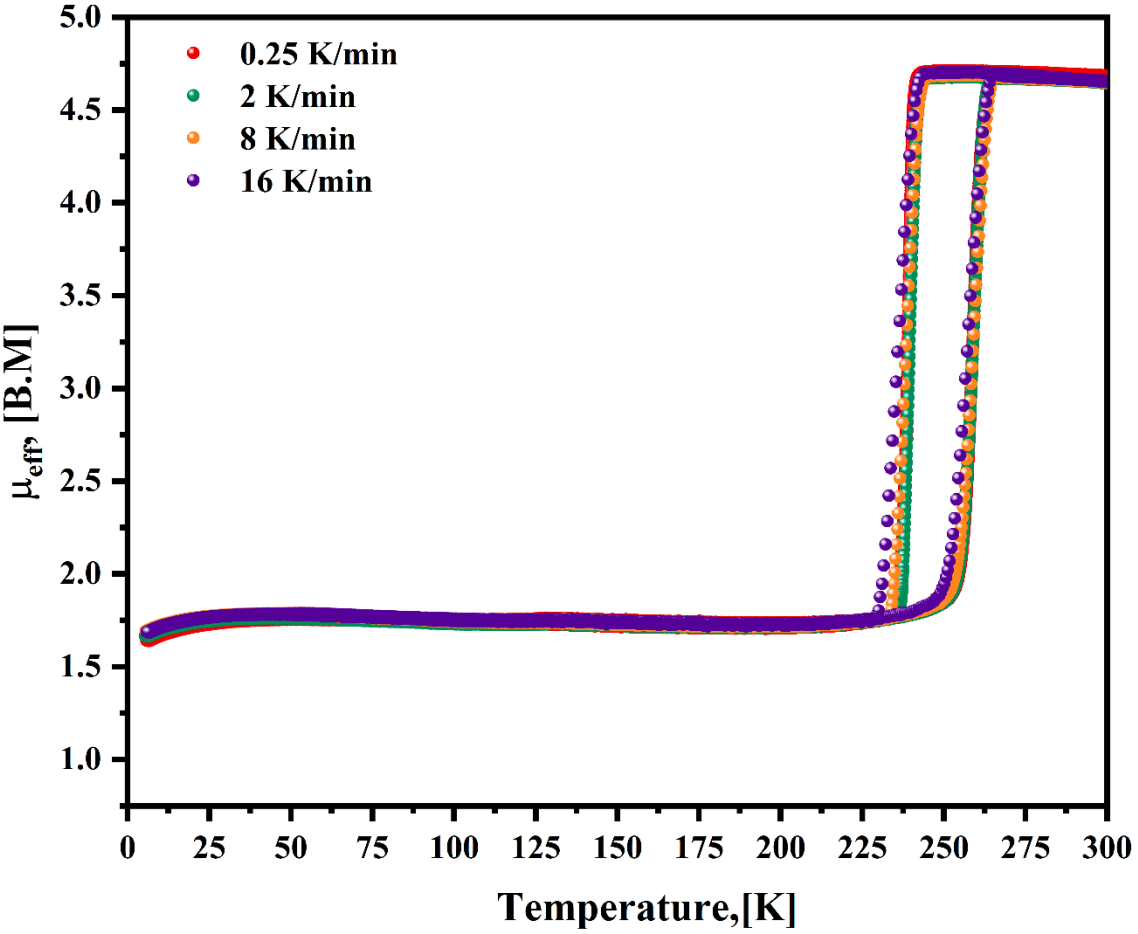

Figure S4. Effective magnetic moment (μ_{eff}) versus temperature of $Fe(4EPy)_2[Fe(CN)_5NO]$, from magnetic data recorded at different values of scan rate in the 6 to 300 K temperature range. Below 25 K, the remaining paramagnetic iron(II) atoms are participating in a weak antiferromagnetic interaction.

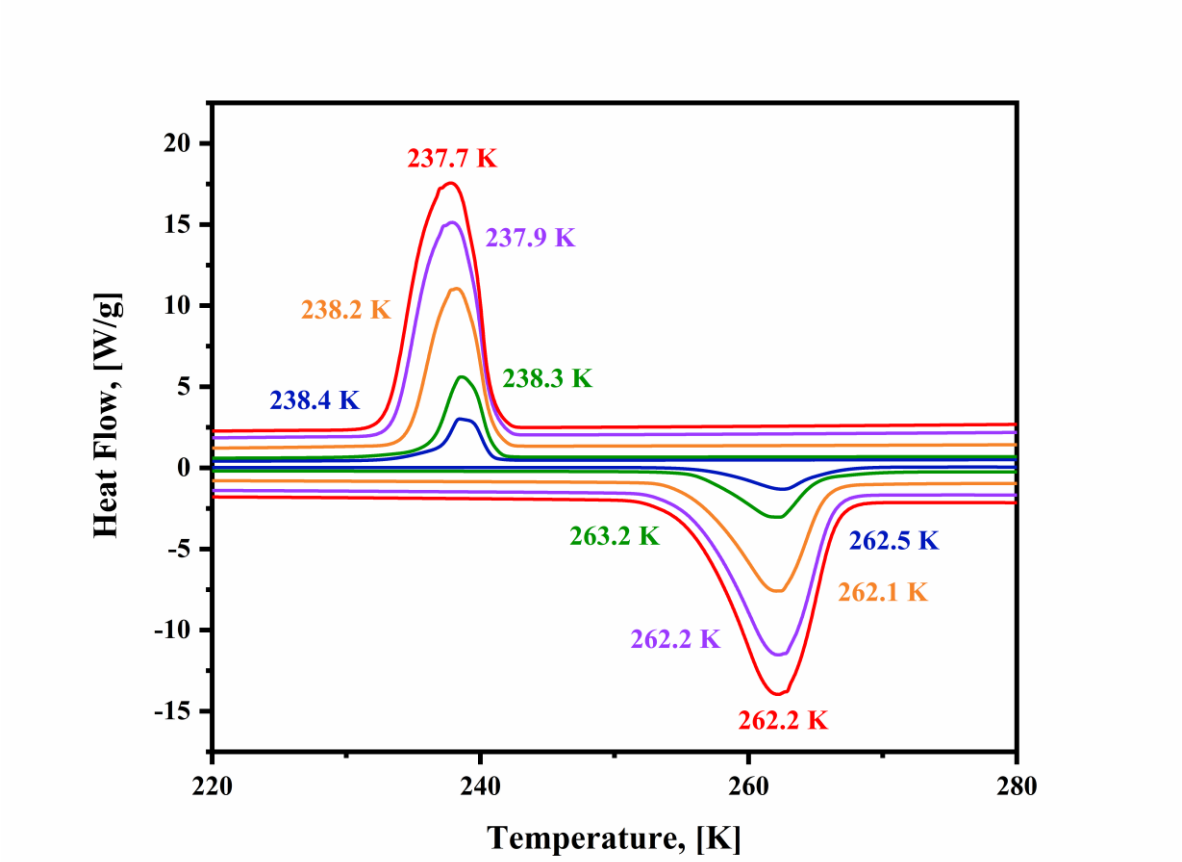

Figure S5. DSC curves of $Fe(4\text{-}EPy)_2[Fe(CN)_5NO]$ using different scan rates, in the temperature region where the spin transitions were observed.

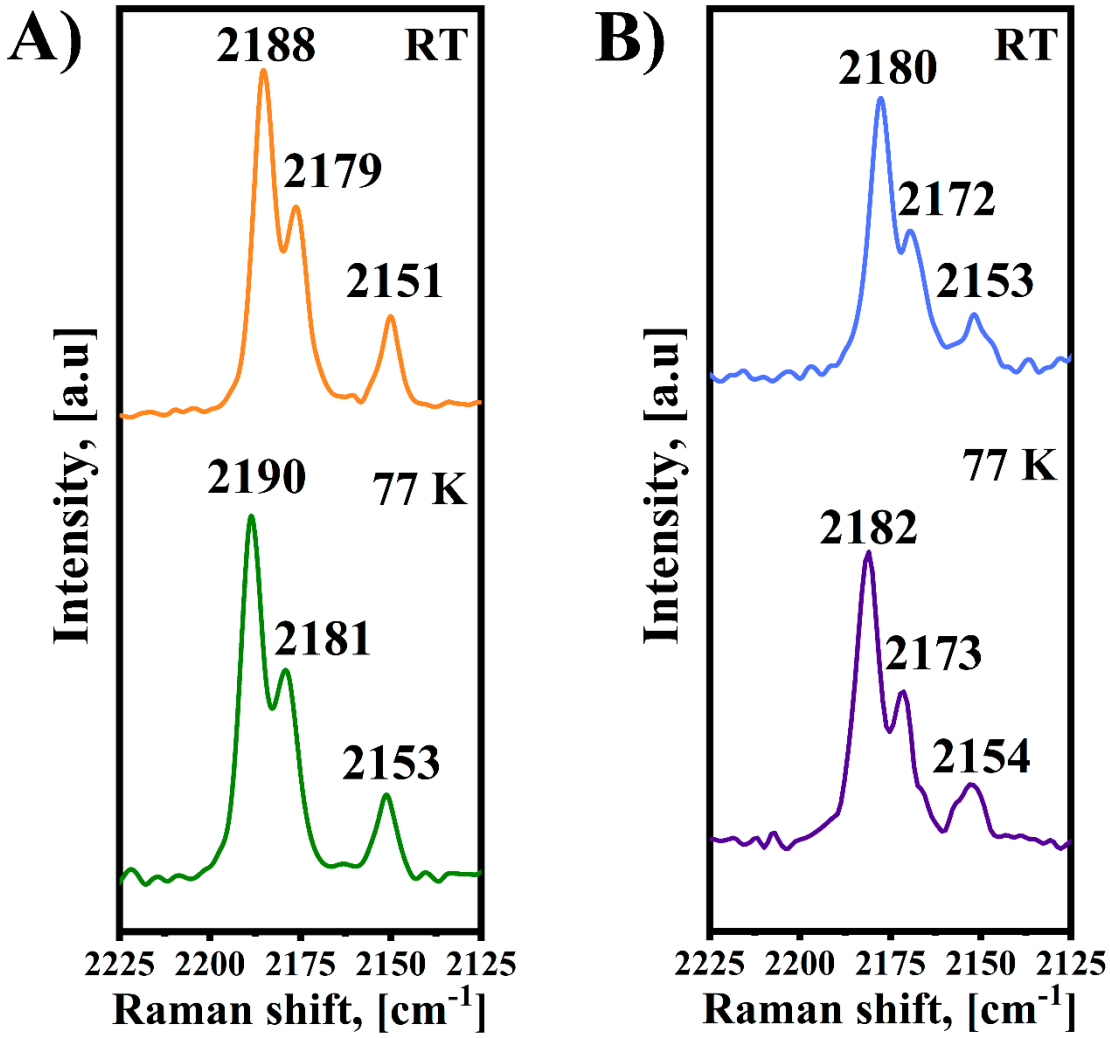

Figure S6. ν(CN) stretching spectral region of the Raman spectra recorded at 77 and 298 K for two pillared ferrous nitroprussides without spin-crossover. A) 3D material: Fe(1,2-Bis(4-Pyridyl)ethane)$_2$[Fe(CN)$_5$NO] and B) 2D material: Fe(4-Phenylpyridine)$_2$[Fe(CN)$_5$NO].

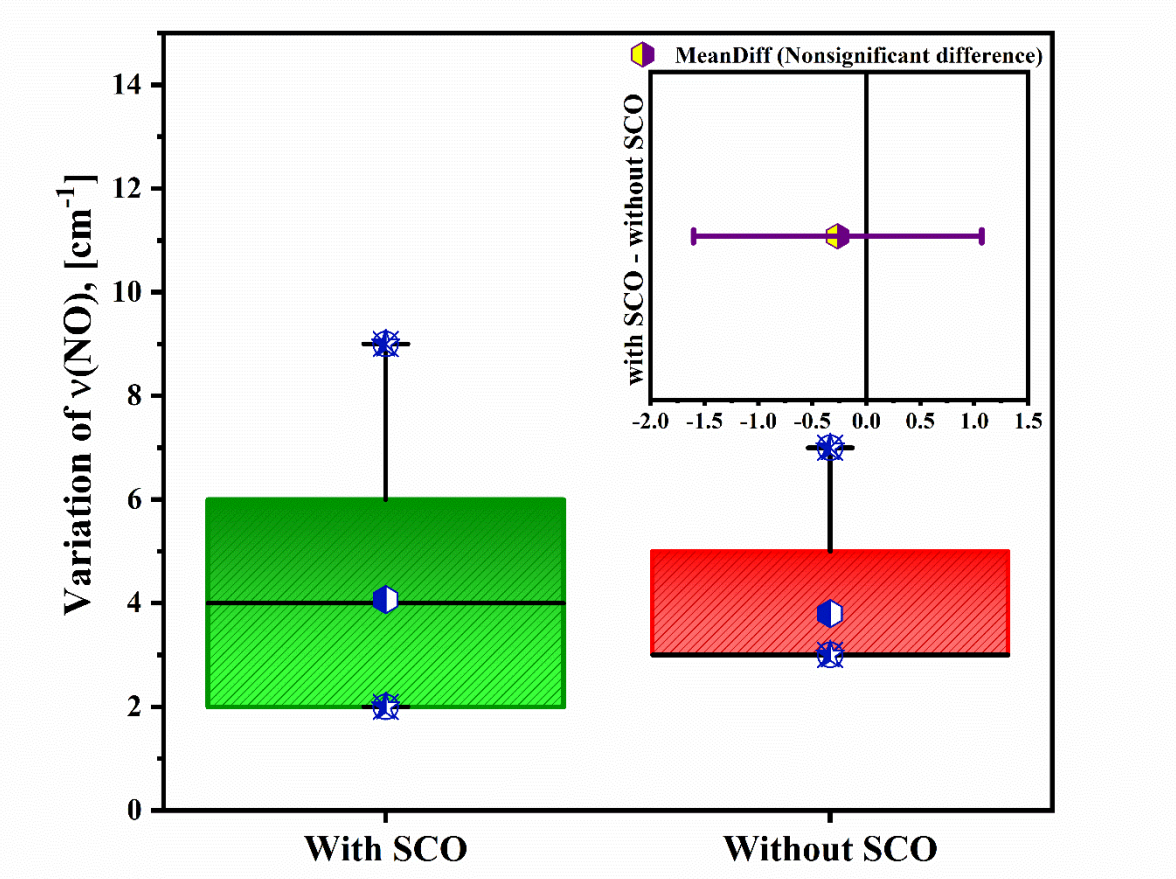

Figure S7. ANOVA analysis of the variation of ν(NO) in pillared 2D ferrous nitroprussides with and without spin crossover.

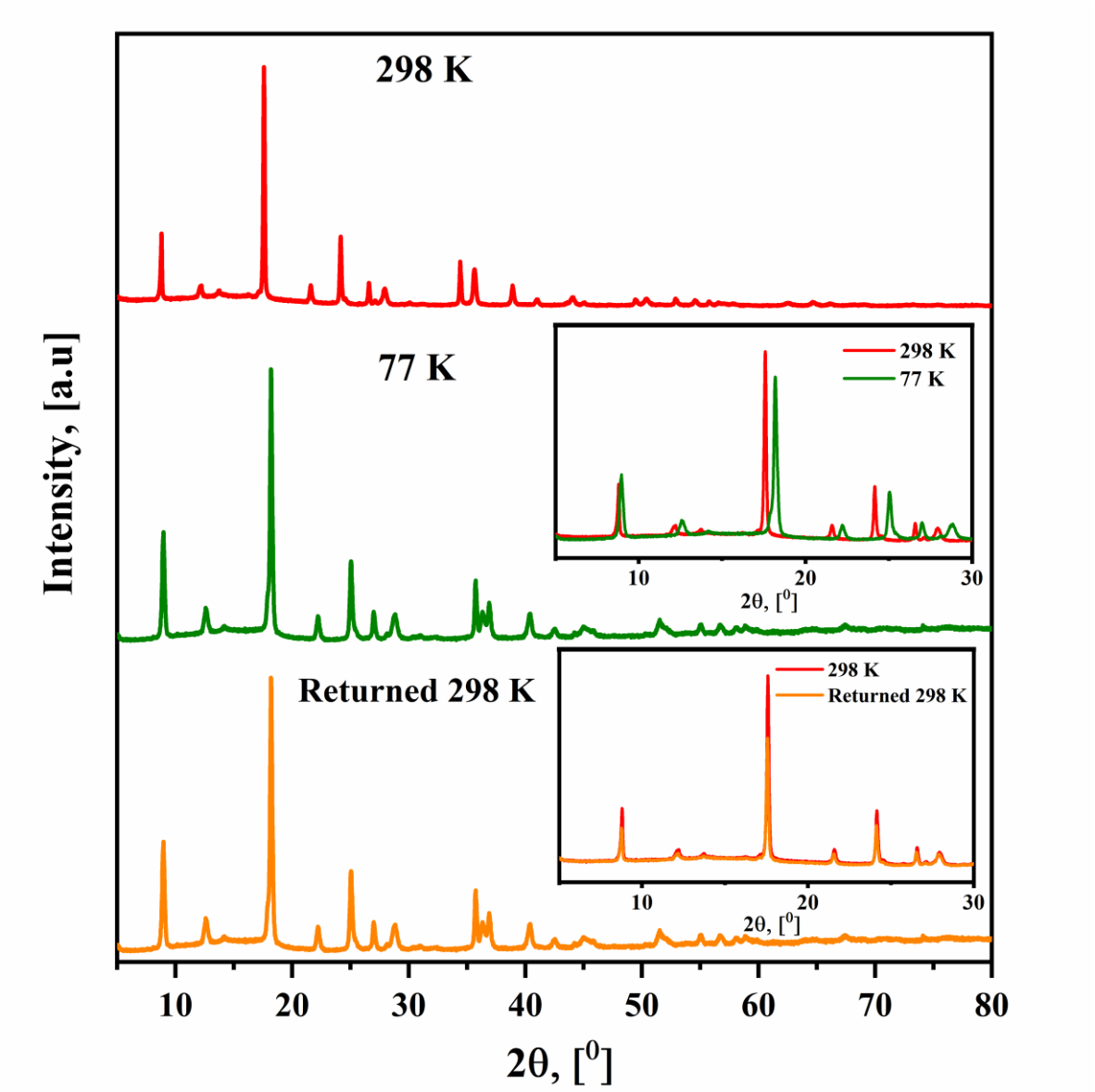

Figure S8. PXRD patterns for $Fe(4EPy)_2[Fe(CN)_5NO]$ recorded at 298 K, 77 K, and then on the sample warming to room temperature (298 K). These patterns were recorded with CuKα radiation using a D8 Advance diffractometer from Bruker.

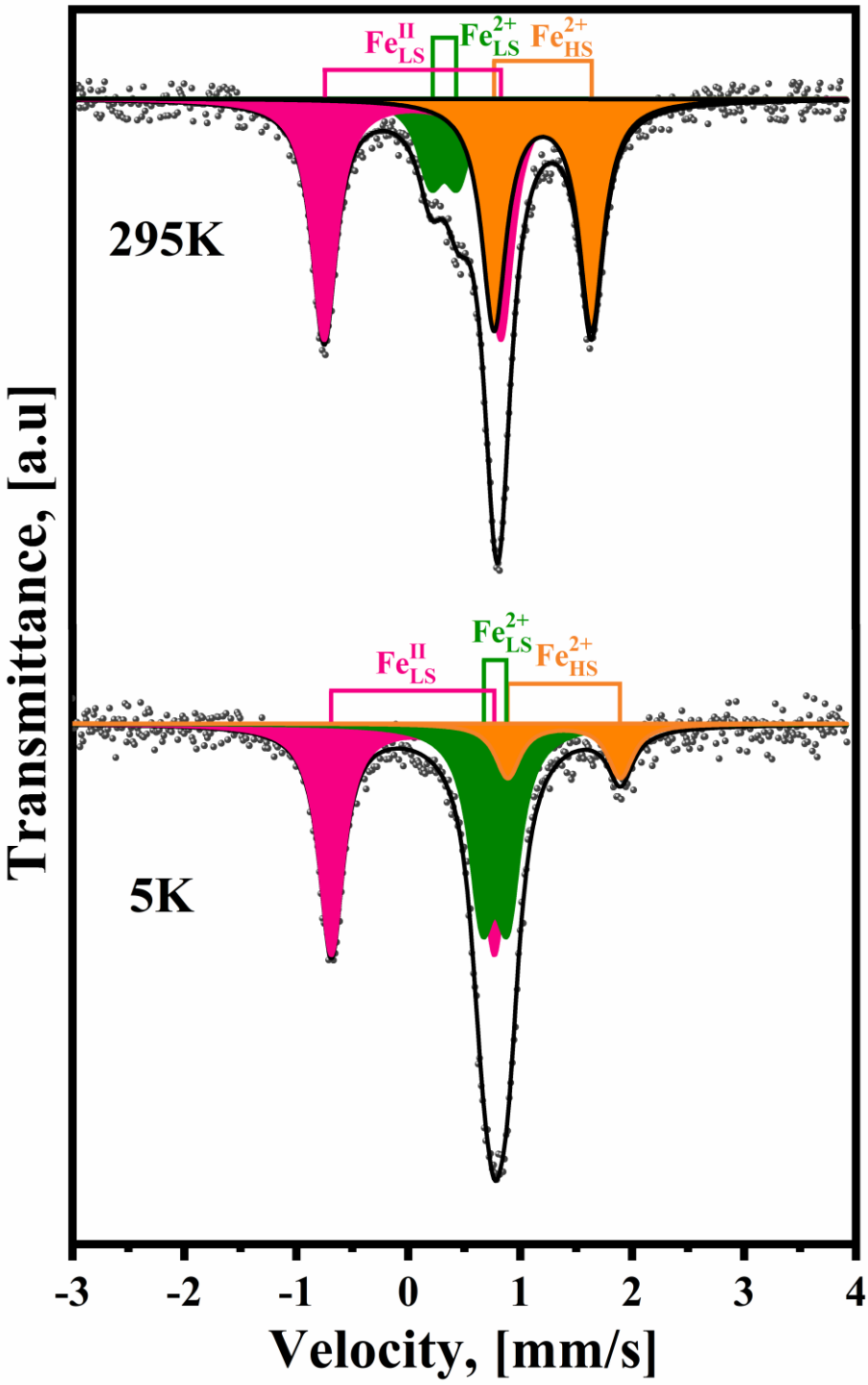

Figure S9. Mössbauer spectra recorded at 295 and 5 K of the $Fe(Quinazoline)_2[Fe(CN)_5NO]$. Labels: A: $Fe^{II}LS$: low spin iron atom (II) in the $[Fe(CN)_5NO]$ block; B: $Fe^{II}HS$: high spin iron atom (II) with $Fe(NC)_4(N_L)_2$ coordination environment; C: $Fe^{II}LS$: low spin iron atom (II) with $Fe(NC)_4(N_L)_2$ coordination. Δ_{QS} (295 K) = 1.578 mm/s; Δ_{QS} (5 K) = 1.457 mm/s; δ (295 K) = 0.040 mm/s and δ (5 K) = 0.041 mm/s. This material shows an incomplete HS $\rightarrow$ LS transition on the sample cooling.

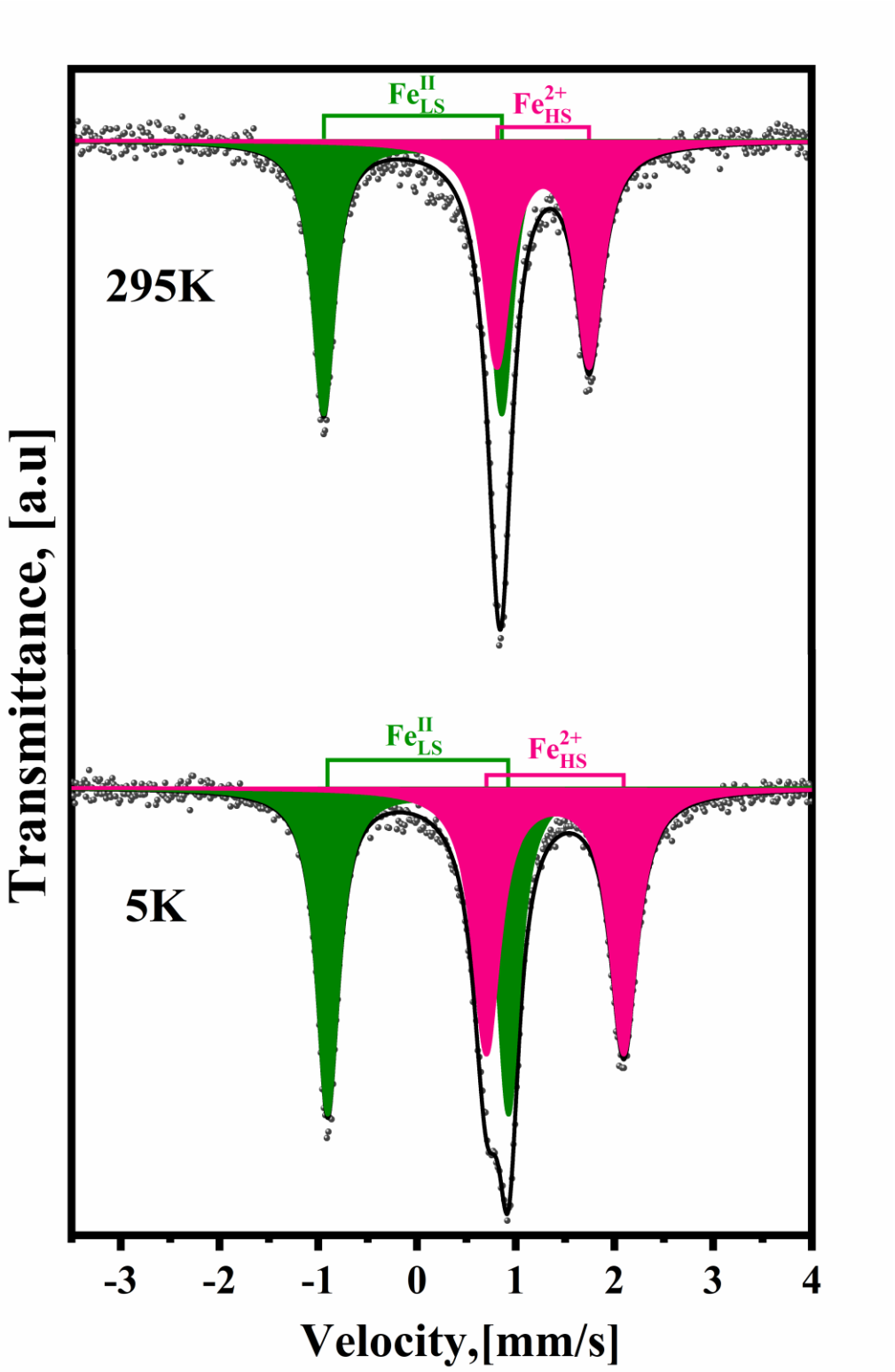

Figure S10. Mössbauer spectra recorded at 295 and 5 K of the Fe(4-Phenylpyridine)$_2$[Fe(CN)$_5$NO]. Labels: A: Fe^{II}LS: low spin iron atom (II) in the [Fe(CN)$_5$NO] block and B: Fe^{II}HS: high spin iron atom (II) with Fe(NC)$_4$(N$_L$)$_2$ coordination environment. This material is free of HS $\rightarrow$ LS transition on the sample cooling.

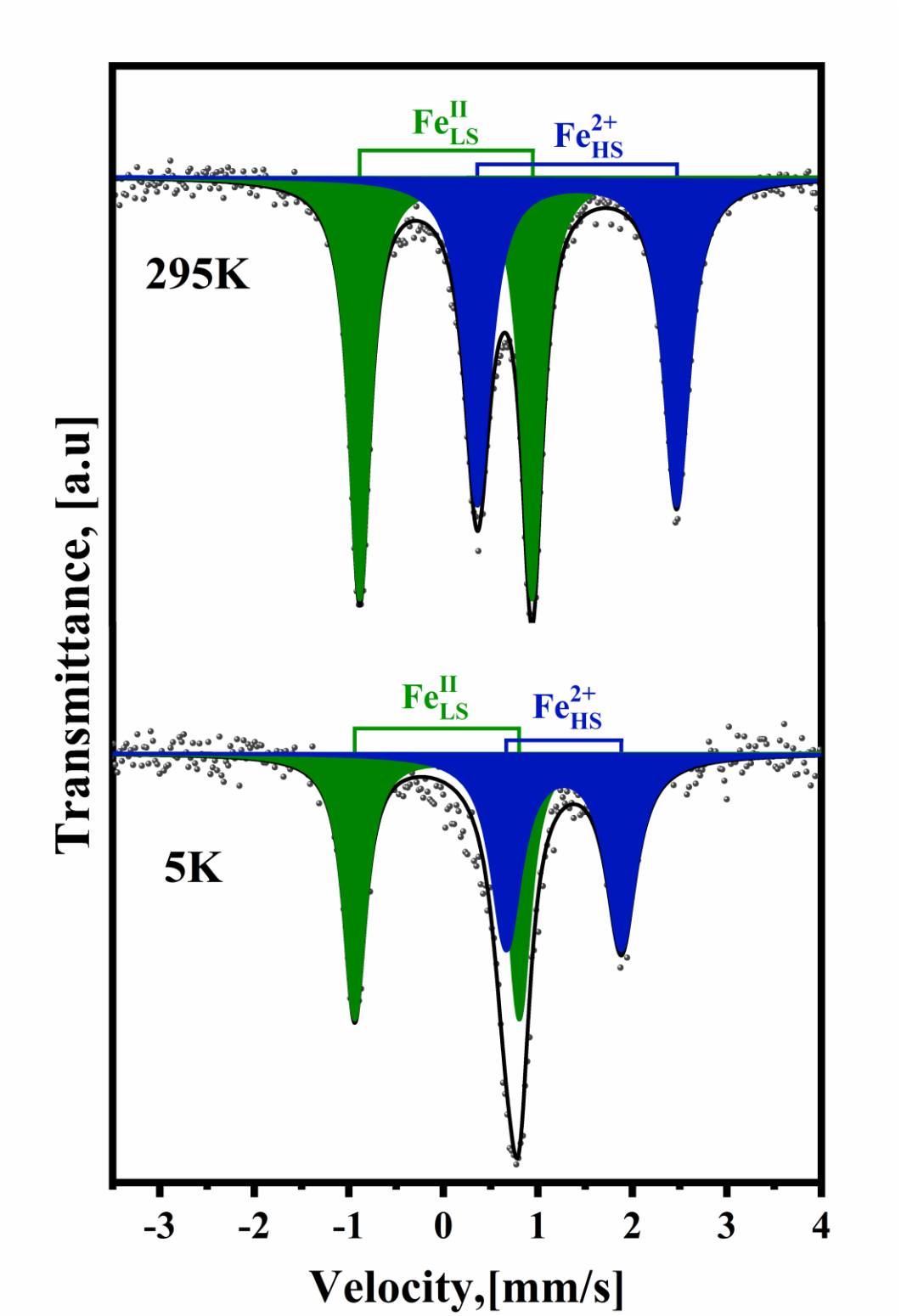

Figure S11. Mössbauer spectra recorded at 295 and 5 K of the Fe(4-Styrylpyridine)$_2$[Fe(CN)$_5$NO]. Labels: A: Fe^{II}LS: low spin iron atom (II) in the [Fe(CN)$_5$NO] block and B: Fe^{II}HS: high spin iron atom (II) with Fe(NC)$_4$(N$_L$)$_2$ coordination environment. This material is free of HS $\rightarrow$ LS transition on the sample cooling.

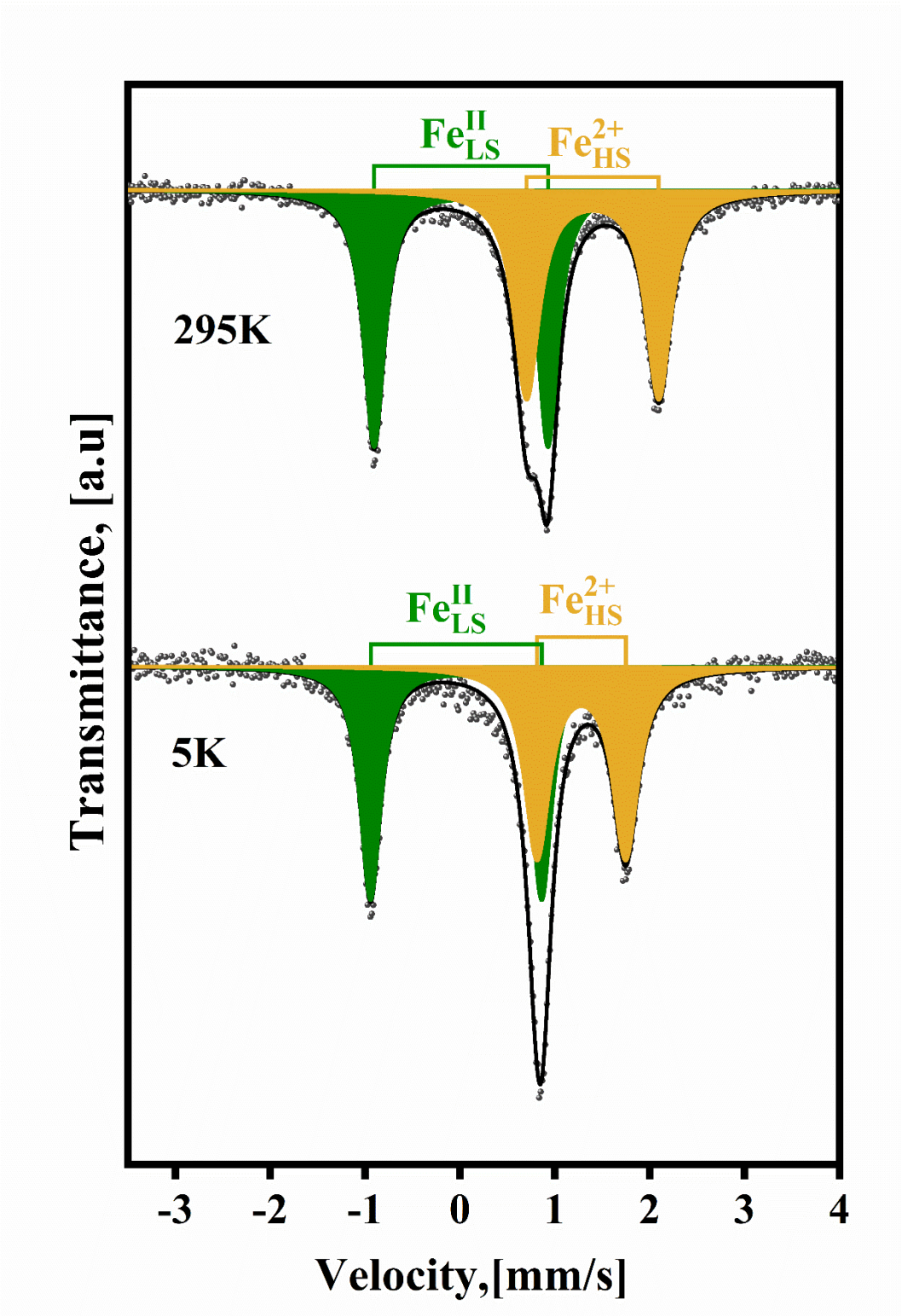

Figure S12. Mössbauer spectra recorded at 295 and 5 K of the Fe(1,10-Phenanthroline)$_2$[Fe(CN)$_5$NO]. Labels: A: Fe^{II}LS: low spin iron atom (II) in the [Fe(CN)$_5$NO] block and B: Fe^{II}HS: high spin iron atom (II) with Fe(NC)$_4$(N$_L$)$_2$ coordination environment. This material is free of HS $\rightarrow$ LS transition on the sample cooling.

Table S3. Details of the refined crystal structure by the Rietveld method.

Composition	**$Fe(4\text{-}EPy)_2[Fe(CN)_5NO]$ at 293 K**	**$Fe(4\text{-}EPy)_2[Fe(CN)_5NO]$ 190 K**
Data collection		
Diffractometer	magnet beamline 08B1-1 Pilatus3 S 6M detector	
Wavelength (Å)	18 keV (λ = 0.6868 Å)	
2θ range (°)	5.06141- 50.00475	
Crystal data		
Empirical formula	$Fe_4\ C_{38}\ N_{16}\ O_2\ H_{28}$	
Empirical formula weight	964.133 g/mol	
Crystal system	Orthorhombic	
Space group	C m m m (65)	
Unit cell dimensions	a = 20.1476(10) Å	a=19.7722(10) Å
	b = 7.3815(10) Å	b=7.104(1) Å
	c = 7.3601(10) Å	c=7.0932(10) Å
	a/b=2.7295 b/c=1.0029 c/a=0.3653	a/b=2.7832 b/c=1.0015 c/a=0.3587
Volume ($Å^3$)	1094.59(22)	996.32(20)
Z	2	
Calculated Density (g/cm^3)	1.46254	

Table S4. Atomic coordinates, isotropic thermal factors, and occupation factors for the refined crystal structures.

Atom	**Ox.**	**Wyck.**	**Site**	**S.O.F.**	**x/a**	**y/b**	**z/c**	**U [$Å^2$]**
$Fe(4EPy)_2[Fe(CN)_5NO]$ at 293 K								
Fe1		2d	mmm		0	0	1/2	0.0390
Fe2		2b	mmm		0	1/2	0	0.0410
C1		8n	m..		0	0.17410	0.30330	0.0500
N1		8n	m..		0	0.27800	0.18990	0.0500
C2		4h	2mm	0.5	-0.09620	0	1/2	0.0500
N2		4h	2mm	0.5	-0.15250	0	1/2	0.0500
N3		4h	2mm	0.5	-0.08430	0	1/2	0.0500
O1		4h	2mm	0.5	-0.14000	0	1/2	0.0500
N4		4g	2mm		0.09170	1/2	0	0.0450
C3		8o	.m.		0.12360	1/2	-0.17580	0.0540
H3		8o	.m.		0.09900	1/2	-0.27740	0.0000
C4		8o	.m.		0.19240	1/2	-0.18370	0.0540
H4		8o	.m.	2	0.21430	1/2	-0.29080	0.0000
C5		4g	2mm		0.22850	1/2	0	0.0540
C6		4g	2mm		0.29970	1/2	0	0.0540
C7		4g	2mm		0.35980	1/2	0	0.0540
H7		4g	2mm		0.40610	1/2	0	0.0000

$Fe(4EPy)_2[Fe(CN)_5NO]$ at 190 K								
Fe1		2d	mmm		0	0	1/2	0.0390
Fe2		2b	mmm		0	1/2	0	0.0410
C1		8n	m..		0	0.18040	0.29610	0.0500
N1		8n	m..		0	0.28840	0.17830	0.0500
C2		4h	2mm	0.5	-0.09790	0	1/2	0.0500
N2		4h	2mm	0.5	-0.15530	0	1/2	0.0500
N3		4h	2mm	0.5	-0.08540	0	1/2	0.0500
O1		4h	2mm	0.5	-0.14180	0	1/2	0.0500
N4		4g	2mm		0.09170	1/2	0	0.0450
C3		8o	.m.		0.12360	1/2	-0.17580	0.0540
H3		8o	.m.		0.09900	1/2	-0.27740	0.0000
C4		8o	.m.		0.19240	1/2	-0.18370	0.0540
H4		8o	.m.		0.21430	1/2	-0.29080	0.0000
C5		4g	2mm		0.22850	1/2	0	0.0540
C6		4g	2mm		0.29970	1/2	0	0.0540
C7		4g	2mm		0.35980	1/2	0	0.0540
H7		4g	2mm		0.40610	1/2	0	0.0000
Fe1		2d	mmm		0	0	1/2	0.0390

Table S5: Selected bond distances and angles for the refined crystal structures.

Composition	**Atoms**	**Bond distance (Å)**	**Atoms**	**Bond angle (°)**
$Fe(4EPy)_2[Fe(CN)_5NO]$ at 293 K	Fe1-C1	1.936(2)	Fe1-C1-N1	179.0(9)
	Fe1-C2	1.938(1)	Fe1-C2-N2	180.0(5)
	Fe1-N3	1.698(1)	Fe1-N3-O1	180.00(2)
	C1-N1	1.133(3)	Fe2-N1-C1	173.04(5)
	C2-N2	1.134(1)	N4-Fe2-N4	180.00 (1)
	N3-O1	1.122(1)	N1-Fe2-N1	180.00 (1)
	Fe2-N1	2.154(3)	N1-Fe2-N1	99.08(3)
	Fe2-N4	1.847(1)	N1-Fe2-N1	80.92(4)
$Fe(4EPy)_2[Fe(CN)_5NO]$ at 190 K	Fe1-C1	1.933(4)	Fe1-C1-N1	178.97(7)
	Fe1-C2	1.936(1)	Fe1-C2-N2	180.0(5)
	Fe1-N3	1.688(1)	Fe1-N3-O1	180.00(2)
	C1-N1	1.134(1)	Fe2-N1-C1	172.63(7)
	C2-N2	1.135(1)	N4-Fe2-N4	180.00 (1)
	N3-O1	1.115(2)	N1-Fe2-N1	180.00 (1)
	Fe2-N1	1.964(1)	N1-Fe2-N1	99.85(4)
	Fe2-N4	1.813(1)	N1-Fe2-N1	80.15(4)

Table S6. Data collection of the frequency for the ν(CN) and ν(NO) absorption bands at 77 K and 295 K, the difference between them, and the dimensionality of materials with spin-crossover.

Ligand	ν(CN), [cm^{-1}] at 295 K	ν(CN), [cm^{-1}] at 77 K	Δ ν(CN), [cm^{-1}]	ν(NO), [cm^{-1}] at 295 K	ν(NO), [cm^{-1}] at 77 K	Δ ν(NO), [cm^{-1}]	Dimensionality
Pyrazine	2176	2188	12	1921	1923	2	3D
4,4'-Azopyridine	2171	2188	17	1926	1933	7	3D
Pyridine	2176	2181	5	1929	1932	3	2D
3-Fluoropyridine	2176	2181	5	1897	1899	2	2D
4-Methylpyridine	2179	2184	5	1934	1936	2	2D
4-Pyridinecarboxaldehyde	2179	2185	6	1936	1938	2	2D
4-Acetylpyridine	2168	2173	5	1898	1904	6	2D
4-Vinylpyridine	2175	2180	5	1926	1933	7	2D
4-(3-Phenylpropyl)propyl	2174	2183	9	1915	1920	5	2D
Quinazoline	2175	2180	5	1918	1922	4	2D
4-Chloropyridine	2181	2186	5	1899	1903	4	2D
4-Iodopyridine	2173	2178	5	1903	1907	4	2D
4-Bromopyridine	2179	2184	5	1900	1902	2	2D
4-Ethynylpyridine	2179	2188	9	1910	1916	6	2D

Table S7. Data collection of the frequency for the ν(CN) and ν(NO) absorption bands at 77 K and 295 K, the difference between them, and the dimensionality of materials without spin-crossover.

Ligand	ν(CN) [cm^{-1}] at 295 K	ν(CN), [cm^{-1}] at 77 K	Δ ν(CN), [cm^{-1}]	ν(NO), [cm^{-1}] at 295 K	ν(NO), [cm^{-1}] at 77 K	Δ ν(NO), [cm^{-1}]	Dimensionality
1,2-Bis(4-pyridyl)ethane	2175	2178	3	1912	1915	3	3D
3-Methylpyridine	2173	2175	2	1916	1919	3	2D
3-Pyridinecarboxaldehyde	2173	2176	3	1921	1924	3	2D
4-Phenylpyridine	2166	2168	2	1909	1912	3	2D
Isoquinoline	2169	2172	3	1901	1904	3	2D

1-vinyl-1,2,4-triazole	2177	2180	3	1922	1927	5	2D
4-Ethylpyridine	2168	2171	3	1901	1905	4	2D
Imidazo [1,2-a]pyridine	2166	2169	3	1917	1920	3	2D
Imidazo [1,2-a]pyrazine	2153	2155	2	1925	1928	5	2D
3-Cyanopyridine	2173	2175	2	1934	1937	3	2D
3-Hidroxypyridine	2174	2177	3	1924	1929	5	2D
Imidazole	2183	2186	3	1939	1946	7	2D
Isonicotinic Acid	2169	2172	3	1925	1928	3	2D
EthylNicotinate	2169	2172	3	1911	1917	6	2D

Table S8. Mössbauer quadrupole splitting (Δ_{QS}) in pillared ferrous nitroprussides with thermally-induced spin-crossover.

Ligand	T (K)	Δ_{QS}(mm/s)	δ*(mm/s)	Reference
Pyridine	295	1.812	-0.083	[a]
	5	1.796	-0.016	[a]
3-Fluoropyridine	295	1.813	-0.021	[b]
	5	1.805	0.067	[b]
4-Acetylpyridine	295	1.833	0.017	[c]
	5	1.762	0.070	[c]
4-Pyridinecarboxaldehyde	295	1.901	-0.021	[c]
	5	1.892	0.075	[c]
4-Methylpyridine	295	1.875	-0.047	[c]
	5	1.587	0.059	[c]
4-Vinylpyridine	295	1.862	-0.038	[c]
	5	1.847	0.072	[c]
4-Chloropyridine	295	1.798	-0.039	[d]
	5	1.489	0.068	[d]
4-Bromopyridine	295	1.823	-0.010	[d]
	5	1.513	0.021	[d]
4-Iodopyridine	295	1.807	-0.023	[d]
	5	1.542	0.014	[d]
Quinazoline	295	1.578	0.040	Figure S6
	5	1.457	0.041	Figure S6
4-Ethynylpyridine	295	1.607	0.013	Figure 3
	5	1.461	0.020	Figure 3

References: [a] *Eur. J. Inorg. Chem*., **2019**, 4966–4973. https://doi.org/10.1002/ejic.201900837; [b] J. *Solid State Chem*. **2020**, 286, 121293. https://doi.org/10.1016/j.jssc.2020.121293; [c] *New J Chem*. **2020**, 44, 5937–46. https://doi.org/10.1039/D0NJ00595A; [d] *New J Chem*. **2022**, 47, 238-249. https://doi.org/10.1039/D2NJ05141A

Table S9. Mössbauer quadrupole splitting (Δ_{QS}) in pillared ferrous nitroprussides without thermally induced spin-crossover.

Ligand	T (K)	Δ_{QS}(mm/s)	δ*(mm/s)	Reference
3-Chloropyridine	295	1.808	-0.064	[b]
	5	1.858	0.076	[b]
3-Bromopyridine	295	1.848	0.024	[b]
	5	1.851	0.075	[b]
3-Iodopyridine	295	1.807	-0.023	[b]
	5	1.836	0.065	[b]
1,3-Oxazole	295	1.772	-0.013	[e]
	5	1.848	0.002	[e]
1H-Pyrazole	295	1.860	-0.014	[e]
	5	1.879	0.088	[e]
Imidazo [1,2-a]pyridine	295	1.789	-0.129	[e]
	5	1.850	-0.003	[e]
1,2-Bis(4-pyridyl)ethane	295	1.885	-0.021	[e]
	5	1.903	0.057	[e]
4-Phenylpyridine	295	1.794	-0.045	Figure S7
	5	1.826	-0.013	Figure S7
4-Styrylpyridine	295	1.757	-0.071	Figure S8
	5	1.827	0.022	Figure S8
1,10-Phenanthroline	295	1.638	-0.158	Figure S9
	5	1.733	-0.047	Figure S9

References: [b] J. *Solid State Chem*. **2020**, 286, 121293. https://doi.org/10.1016/j.jssc.2020.121293; [e] *J Coord Chem* **2021**, 434, 213764. https://doi.org/10.1080/00958972.2020.1870682